Cell Reports
Report

Regulation of Chandelier Cell Cartridge and Bouton Development via DOCK7-Mediated ErbB4 Activation

Yilin Tai,[1] Justyna A. Janas,[1,2,3] Chia-Lin Wang,[1,3] and Linda Van Aelst[1,*]
[1]Cold Spring Harbor Laboratory, Cold Spring Harbor, NY 11724, USA
[2]Present address: Department of Pathology, Institute for Stem Cell Biology and Regenerative Medicine, Stanford University School of Medicine, Stanford, CA 94305, USA
[3]These authors contributed equally to this work
*Correspondence: vanaelst@cshl.edu
http://dx.doi.org/10.1016/j.celrep.2013.12.034
This is an open-access article distributed under the terms of the Creative Commons Attribution-NonCommercial-No Derivative Works License, which permits non-commercial use, distribution, and reproduction in any medium, provided the original author and source are credited.

SUMMARY

Chandelier cells (ChCs), typified by their unique axonal morphology, are the most distinct interneurons present in cortical circuits. Via their distinctive axonal terminals, called cartridges, these cells selectively target the axon initial segment of pyramidal cells and control action potential initiation; however, the mechanisms that govern the characteristic ChC axonal structure have remained elusive. Here, by employing an in utero electroporation-based method that enables genetic labeling and manipulation of ChCs in vivo, we identify DOCK7, a member of the DOCK180 family, as a molecule essential for ChC cartridge and bouton development. Furthermore, we present evidence that DOCK7 functions as a cytoplasmic activator of the schizophrenia-associated ErbB4 receptor tyrosine kinase and that DOCK7 modulates ErbB4 activity to control ChC cartridge and bouton development. Thus, our findings define DOCK7 and ErbB4 as key components of a pathway that controls the morphological differentiation of ChCs, with implications for the pathogenesis of schizophrenia.

INTRODUCTION

The maturation and function of cortical networks depend on intricate interactions between glutamatergic pyramidal neurons (PyNs) and GABAergic interneurons. PyNs are typically specialized to transmit information across cortical layers and regions, and interneurons play important roles in controlling and shaping the output of local PyNs. Therefore, interneurons are essential to the function, complexity, and computational architecture of neural circuits (Batista-Brito and Fishell, 2009; Huang et al., 2007; Marín, 2012). Among the various interneuron subtypes, chandelier cells (ChCs) in particular are believed to have powerful control over the output of PyNs, owing to their unique morphology and type of connections they make (Howard et al., 2005; Somogyi, 1977; Woodruff et al., 2010). Indeed, ChCs possess a very distinctive axonal arbor with multiple arrays of short vertical sets of cartridges, each harboring a string of synaptic boutons (Howard et al., 2005; Inda et al., 2009). This unique architecture enables a single ChC to couple to a large population of PyNs. Furthermore, ChCs selectively innervate the axon initial segment (AIS) of PyNs (DeFelipe et al., 1985; Somogyi, 1977), the most excitable part of a neuron where the action potential is initiated (Ogawa and Rasband, 2008). Together, these characteristics make ChCs ideally suited to exert powerful control over the spiking of a large group of PyNs.

In concurrence with an important role for ChCs in controlling cortical network activity, changes in ChC cartridges/boutons and/or function have been reported in disease states such as schizophrenia (DeFelipe, 1999; Lewis, 2012). For instance, a decrease in ChC cartridge and/or bouton density in the prefrontal cortex of individuals with schizophrenia has been described (Pierri et al., 1999; Woo et al., 1998). To date, however, details on ChC cartridge/bouton development and synaptic arborization remain scarce (Fish et al., 2013; Inan et al., 2013; Taniguchi et al., 2013), and little is known about the molecular mechanisms that govern the morphological differentiation and functional maturation of ChCs (Fazzari et al., 2010). The main obstacles have been a lack of unique biochemical ChC markers and versatile methods to target and manipulate gene expression in these cells.

In recent studies examining the expression patterns of members of the DOCK180 family, an atypical class of Rac and/or Cdc42 GTPase guanine nucleotide exchange factors (GEFs) (Côté and Vuori, 2002; Meller et al., 2005; Miyamoto and Yamauchi, 2010), in GABAergic interneurons, we intriguingly observed the presence of the DOCK7 family member, among other parvalbumin (PV)-expressing interneurons, in ChCs of adolescent/adult mouse brains. DOCK7 was previously shown to control the polarization and genesis of newborn pyramidal neurons by promoting Rac activity and antagonizing TACC3 (transforming acidic coiled-coil-containing protein 3) function, respectively

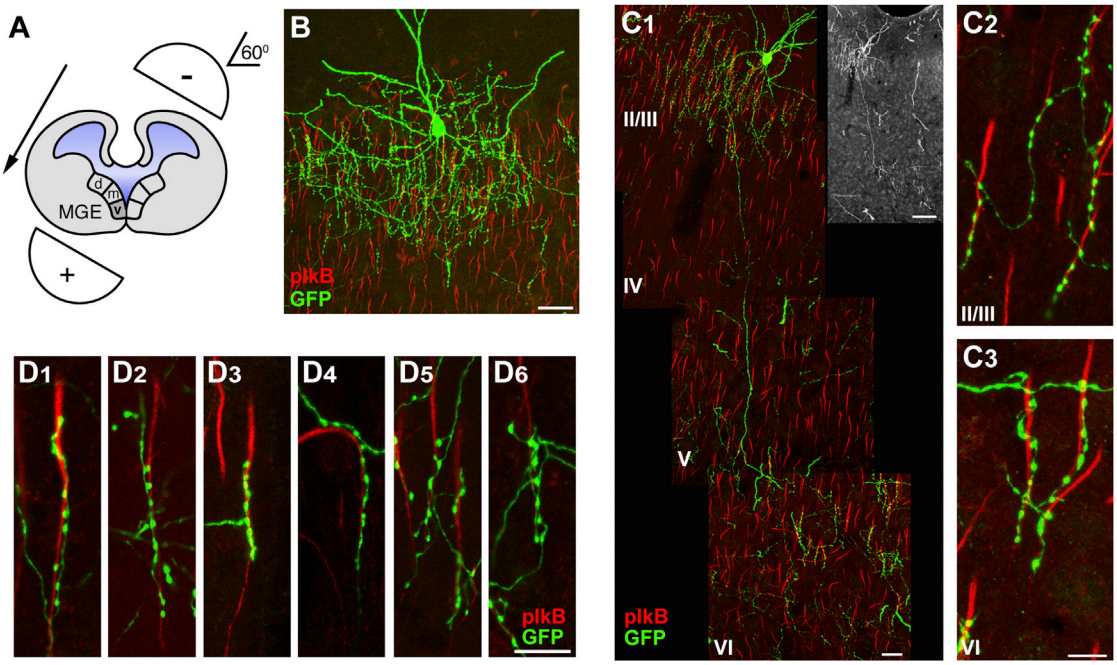

Figure 1. Delivery of Gene Expression to ChCs by In Utero Electroporation

(A) Schematic drawing depicting the ~60° angle of incline of electrode paddles with respect to the horizontal plane of the fetus's brain used to direct DNA transfection toward the ventral medial ganglionic eminence (vMGE).

(B) Representative image of ChC in layer II/III of somatosensory cortex from a mouse electroporated at E12.5 with an EGFP-expressing plasmid and sacrificed at P28. Scale bar, 20 μm.

(C) Example of cortical layer II/III ChC extending a single axonal branch into layer VI to innervate AISs of layer VI PyNs. Mouse embryos were electroporated at E12.5 with an EGFP-expressing plasmid and sacrificed at P28. (C_1) Entire view of layer II/III ChC innervating AISs of both layer II/III and layer VI PyNs. Insert on the top, right is a lower magnification of ChC on the left showing intact cell. Scale bars, 20 μm (bottom) and 100 μm (top). (C_2, C_3) Detailed view of cartridges of ChC depicted in (C_1) innervating AISs of layer II/III (C_2) and layer VI (C_3) PyNs. Scale bar, 10 μm.

(D) Representative images of ChC cartridges contacting AIS of PyNs. Scale bar, 10 μm.

AISs of PyNs (in B, C, and D) are visualized by immunostaining with an antibody to phospho-IkappaB (pIkB).

(Watabe-Uchida et al., 2006; Yang et al., 2012). Here, by implementing an in utero electroporation-based method that enables genetic labeling and manipulation of ChCs at single-cell resolution, we demonstrate a key role for DOCK7 in ChC cartridge/bouton development. Furthermore, we show that DOCK7 interacts with and positively modulates the activity of the schizophrenia-associated ErbB4 receptor tyrosine kinase (RTK), a member of the ErbB family whose expression is largely confined to PV-expressing ChCs and basket cells in the cerebral cortex (Del Pino et al., 2013; Fazzari et al., 2010). Most importantly, we present evidence that DOCK7 controls ChC cartridge/bouton development by modulating the activity of ErbB4. Thus, our data unveil a critical role for DOCK7 as a cytoplasmic modulator of ErbB4 activity in the regulation of ChC cartridge/bouton development.

RESULTS

Delivery of Gene Expression to ChCs by Directional In Utero Electroporation

Based on recent evidence indicating that progenitors in the ventral medial ganglionic eminence (vMGE) provide a source of ChCs (Inan et al., 2012; Taniguchi et al., 2013), we reasoned it should be possible to target gene expression in nascent ChCs by means of in utero electroporation directed toward the vMGE. To this end, we introduced an enhanced green fluorescent protein (EGFP) encoding plasmid into the lateral ventricle of embryonic day 12.5 (E12.5) to E13.5 mouse embryos and directed the current and DNA transfection toward the vMGE by placing electrodes at about 60° from the brain's horizontal plane (Figure 1A). Animals that developed from electroporated embryos were sacrificed at postnatal day 28 (P28), when ChCs are fully differentiated, and brain slices analyzed. Strikingly, using this approach we were able to reproducibly transfect and fluorescently label, among some other interneurons, ChCs at single-cell resolution. EGFP-transfected ChCs were detected in the neocortex, archicortex, and amygdala (Figures 1B and S1), consistent with previous immunohistochemical studies (DeFelipe et al., 1985; Inda et al., 2009; McDonald, 1982; Sik et al., 1993; Somogyi et al., 1982).

Within the neocortex, GFP-labeled ChCs were detected in layer II/III, layer V, and layer VI (Figures S1D–S1F), though layer II/III ChCs were most frequently targeted. Indeed, we found that all EGFP-labeled ChCs resided in layers II/III when electroporations were performed at E12.5, and, remarkably, only when electroporations were performed at E13.5, we found about

10% of the labeled ChCs in layers V and VI. Intriguingly, besides innervating AISs of PyNs within the same layer, we noted that some layer II/III ChCs also extended a single axonal branch across different layers reaching as far as layer VI to innervate AISs of layer VI PyNs (Figure 1C). This is of particular interest, as this property could endow ChCs with the ability to synchronize neuronal activity across cortical layers. We further analyzed in more detail the cartridges of layer II/III ChCs. We quantified the average length of the cartridges to be 22.2 ± 6.4 μm (mean ± SEM; n = 64 cartridges from nine ChCs), each containing on average 7.1 ± 2.0 boutons (mean ± SEM; n = 64 cartridges from nine ChCs). The average distance between the bouton located proximal to the cell body on the AIS and the cell body of target PyNs was 10.9 ± 4.4 μm (mean ± SEM; n = 64 cartridges from nine ChCs). Given that overall the length of the AISs of layer II/III mouse cortical neurons is ~30 μm, these findings imply that ChC cartridges preferentially innervate the distal part of the AIS. Noteworthy, while cartridges were generally reported to climb upward along the AIS in a vertical position (Howard et al., 2005; Somogyi et al., 1982), we found that they not only can climb upward, but also descend down the AIS (Figures 1D_1–1D_3), and form contacts with the AIS, despite the AIS not being vertical to the pia (Figure 1D_4). Moreover, the cartridges were often branched (Figure 1D_5), and in rare cases we noted that more than one cartridge (two to three cartridges) from the same GFP-labeled ChC innervated one AIS (Figure 1D_6). Together, these data demonstrate that vMGE-directed in utero electroporation presents a versatile approach to deliver gene expression in ChCs and is well suited for examining ChC morphology at single-cell resolution.

DOCK7 Is Required for ChC Cartridge/Bouton Development

We next tackled the identification of molecular mechanisms that govern ChC cartridge/bouton development. As aforementioned, in studies examining the expression of DOCK180 family members in GABAergic interneurons, we observed the presence of DOCK7, among other PV-expressing interneurons (i.e., basket cells), in ChCs of adolescent/adult mouse brains (Figure S2A; data not shown). This finding prompted us to explore a potential role for DOCK7 in the morphological differentiation of ChCs. To this end, we combined the above-described in utero electroporation approach with RNA interference (RNAi) to knock down endogenous DOCK7 protein levels. For RNAi, we used previously described vectors that express a short hairpin RNA (shRNA) targeting the DOCK7 protein coding sequence (Dock7#1) or the 3′ UTR (Dock7#2) of mouse *DOCK7* mRNA or a control scrambled (scr#1) shRNA (Watabe-Uchida et al., 2006; Yang et al., 2012).

Akin to ChCs expressing EGFP alone, ChCs coexpressing scr#1, Dock7#1, or Dock7#2 shRNA all resided in neocortical layers II/III, when embryos were electroporated at E12.5. Interestingly, although DOCK7 knockdown did not prevent the formation of ChC dendrites and axons, the axonal cartridges of both Dock7#1 and Dock7#2 shRNA-expressing ChCs were disorganized in comparison to those of scr#1 shRNA-expressing ChCs (Figures 2A and 2B; data not shown). This was particularly evident when the electroporated neocortices were coimmunostained with a pIkB antibody, which labels the AIS of neighboring PyNs (Figures 2D and 2E). Also, we found that both Dock7#1 and Dock7#2 shRNA significantly decreased the density and size of boutons compared to scr#1 shRNA (Figures 2A, 2B, 2G, and 2H), whereas no significant difference in cartridge length was observed (Figure S2B). Rescue experiments using DOCK7 cDNA that lacks the 3′ UTR and is therefore resistant to Dock#2 shRNA-mediated RNA interference demonstrated that the effects of DOCK7 RNAi were specific (Figures 2C, 2F, 2G, and 2H). To further establish the requirement of DOCK7 for ChC bouton development, we examined whether knockdown of DOCK7 in ChCs at later developmental stages (after P7–P8) also leads to a decrease in bouton size and density. To this end, we engineered a Cre-dependent inducible RNAi expression vector targeted against DOCK7 (Figures S3A and S3B). This vector was coelectroporated with a vector expressing a tamoxifen-inducible form of Cre recombinase in E12.5 embryos. Tamoxifen was then delivered to pups at P7–P8, and animals were sacrificed at P28 and ChCs analyzed (Figure S3C). We found that also in this case DOCK7 knockdown causes a decrease in bouton size and density, while no apparent axonal phenotype is observed (Figures S3C–S3G), corroborating that DOCK7 is required for proper ChC bouton development. Of note, knockdown of DOCK7 in PV-expressing basket cells (at E12.5, as in Figure 2) did not affect the bouton density of these cells (Figure S2E).

We then examined the effects of DOCK7 overexpression on ChC morphology and essentially observed the opposite phenotypes than those seen for DOCK7 RNAi. An organized network of ChC cartridges was formed, with cartridges innervating AISs of their postsynaptic target cells (Figures 2I–2L). Furthermore, both the density and size of boutons of Flag-DOCK7-expressing ChCs were increased compared to control-vector-expressing cells (Figures 2I, 2J, 2M, and 2N), whereas cartridge length and number was not affected (Figures S2C and S2D). Together, these data unveil a critical role for DOCK7 in ChC cartridge/bouton development.

DOCK7 Is a Cytoplasmic Activator of the ErbB4 Receptor

Besides DOCK7, the only other protein hitherto implicated in ChC bouton formation is the ErbB4 RTK. In particular, recent studies demonstrated a decrease in ChC bouton number in *ErbB4* mutant mice, in which ErbB4 was conditionally deleted in a subset of interneurons (Del Pino et al., 2013; Fazzari et al., 2010). Interestingly, DOCK7 had previously been shown to interact with the ErbB2 family member, playing a role in Schwann cell myelination (Yamauchi et al., 2008). ErbB2, however, in contrast to ErbB4, reportedly is not expressed in PV-expressing basket and ChCs in the cerebral cortex (Birchmeier, 2009; Fazzari et al., 2010). Also, we were unable to detect ErbB2 expression in ChCs (data not shown). Hence, we decided to examine whether DOCK7 also interacts with ErbB4, and found that this is indeed the case. Coimmunoprecipitation experiments using extracts prepared from transiently transfected human embryonic kidney 293 cells (HEK293) cells or mouse Neuro 2A cells demonstrated that ErbB4 specifically coimmunoprecipitated with DOCK7 and, vice versa, that DOCK7 specifically

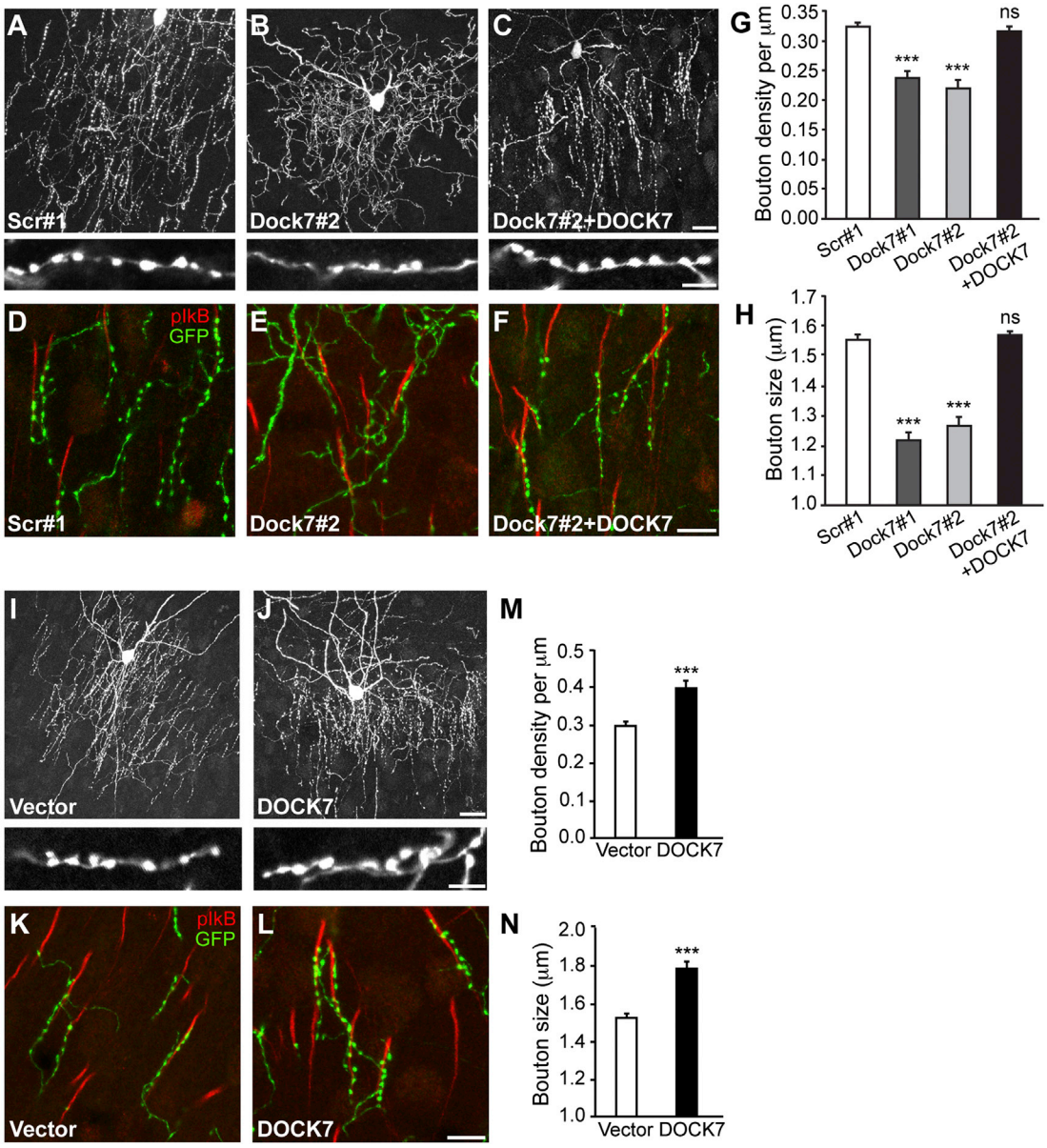

Figure 2. Effects of Altered DOCK7 Expression on ChC Cartridge/Bouton Development

(A–H) DOCK7 knockdown impairs ChC cartridge/bouton development.

(A–C) Representative images of ChCs in layer II/III of somatosensory cortex from mice coelectroporated at E12.5 with plasmids expressing EGFP and scr#1 shRNA, Dock7#2 shRNA, or Dock7#2 RNA + Flag-DOCK7 (DOCK7) and sacrificed at P28. Enlarged view of ChC cartridges with boutons is depicted on bottom. Scale bars, 20 μm (top) and 5 μm (bottom).

(D–F) Representative images illustrating innervation of AISs by cartridges of ChCs transfected with EGFP-expressing plasmid and one of the indicated constructs. The AIS is visualized by immunostaining with an antibody to pIkB. Scale bar, 10 μm.

(G and H) Quantification of bouton density (G) and size (H). Data are mean ± SEM; 7–11 ChCs from three animals were analyzed for each condition, and for each cell 7–15 cartridges (G) and 52–149 boutons (H) were analyzed. ***$p < 0.001$; ns (not significant) indicates $p \geq 0.05$, in comparison to scr#1; one-way ANOVA, post hoc Tukey-Kramer test.

(I and N) Ectopic DOCK7 expression promotes ChC cartridge/bouton development.

(I and J) Representative images of ChCs in layer II/III of somatosensory cortex from mice coelectroporated at E12.5 with plasmids expressing EGFP and empty control vector (vector) or Flag-DOCK7 (DOCK7) and sacrificed at P28. Enlarged view of ChC cartridges with boutons is depicted on the bottom. Scale bars, 20 μm (top) and 5 μm (bottom).

(K and L) Representative images illustrating innervation of AISs by cartridges of ChCs transfected with EGFP-expressing plasmid and one of the indicated constructs. Scale bar, 10 μm.

(M and N) Quantification of bouton density (M) and size (N). Data are mean ± SEM; 11 ChCs from three animals were analyzed for each condition, and for each cell 7–17 cartridges (M) and 54–155 boutons (N) were analyzed. ***$p < 0.001$; Student's t test.

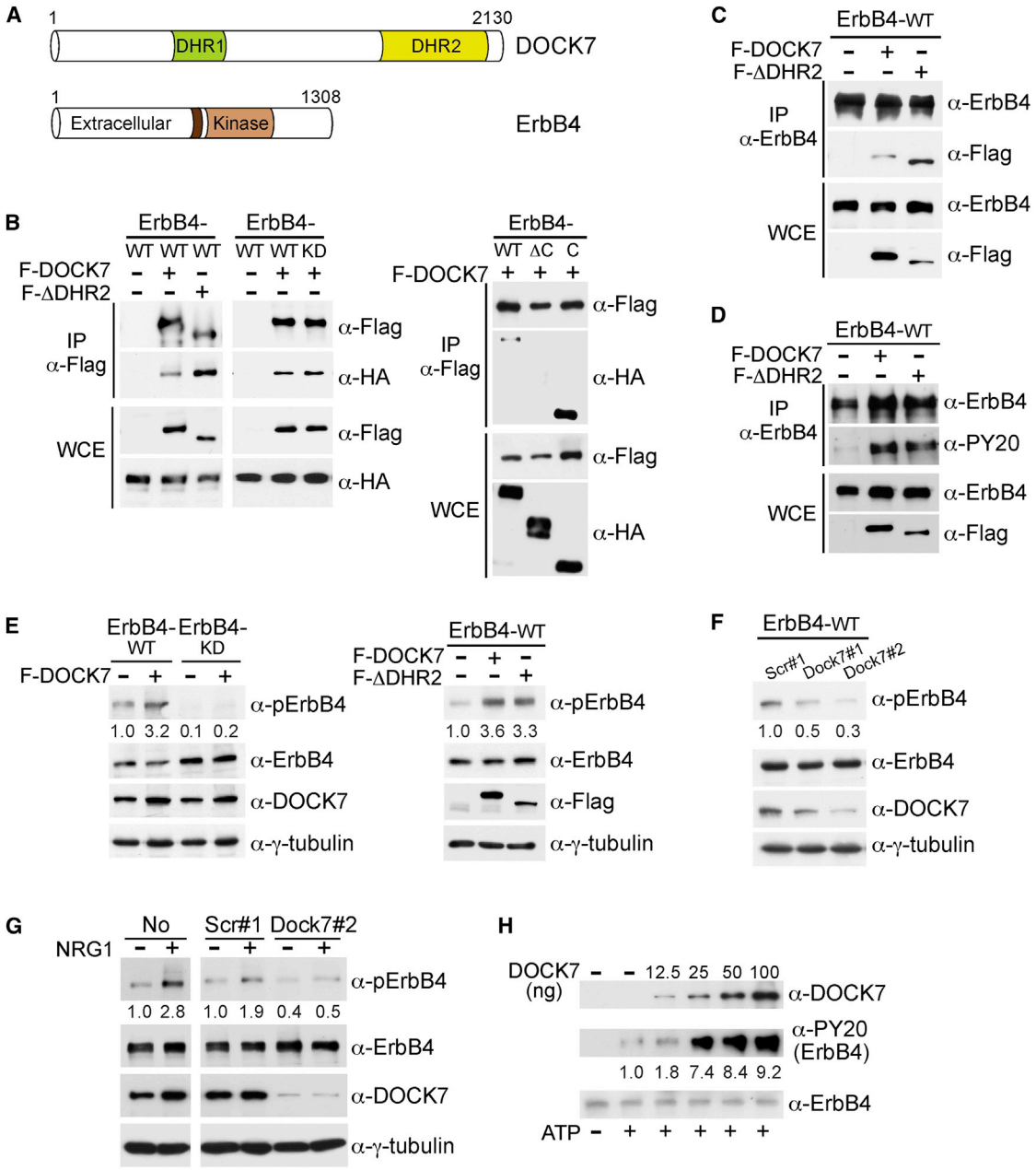

Figure 3. DOCK7 Interacts with and Enhances Activation of ErbB4

(A) Schematic diagram of DOCK7 and ErbB4 domain structure. Dark brown box in ErbB4 represents hydrophobic transmembrane domain.

(B) DOCK7-ErbB4 interaction in human HEK293 cells. Extracts from HEK293 cells transiently expressing wild-type (WT), kinase-dead (K751M; KD), C-terminal deletion mutant (ΔC), or cytoplasmic domain (C) of ErbB4-HA alone or in combination with Flag-DOCK7 (F-DOCK7) or Flag-DOCK7ΔDHR2 (F-ΔDHR2) were immunoprecipitated (IP) with an antibody (Ab) to Flag and analyzed by western blotting with Abs to Flag and HA. WCE, whole cell extract.

(C) DOCK7-ErbB4 interaction in mouse Neuro 2A cells. Extracts from Neuro 2A cells transiently expressing ErbB4 WT alone or in combination with F-DOCK7 or F-ΔDHR2 were immunoprecipitated with an Ab to ErbB4 and analyzed by western blotting with Abs to ErbB4 and Flag.

(D) Ectopic expression of DOCK7 or DOCK7ΔDHR2 increases tyrosine phosphorylation of ErbB4. Extracts from Neuro 2A cells transiently expressing ErbB4 WT alone or in combination with F-DOCK7 or F-ΔDHR2 were immunoprecipitated with an Ab to ErbB4 and analyzed by western blotting with Abs to ErbB4, phosphotyrosine (PY20), and Flag.

(E) Ectopic DOCK7 expression enhances autophosphorylation of WT, but not kinase-dead, ErbB4 and does so independently of its DHR2 domain. Extracts from Neuro 2A cells transiently expressing WT or KD ErbB4 alone or in combination with F-DOCK7 (left) or ErbB4 WT alone or in combination with F-DOCK7 or F-ΔDHR2 (right) were subjected to western blot analysis using Abs to phospho(p)-ErbB4 (Tyr1284), ErbB4, DOCK7, or Flag and to γ-tubulin as a loading control.

(F) Knockdown of DOCK7 decreases autophosphorylation of ectopically expressed ErbB4 in Neuro 2A cells. Extracts from Neuro 2A cells transiently expressing ErbB4 WT together with scr#1, Dock7#1, or Dock7#2 shRNA were subjected to western blot analysis with the indicated Abs.

(legend continued on next page)

coimmunoprecipitated with ErbB4 (Figures 3A–3C). Interestingly, we found that the DHR2 domain of DOCK7, which is conserved among all DOCK180 family members and catalyzes the exchange of GDP for GTP on Rac and/or Cdc42 (Watabe-Uchida et al., 2006; Yamauchi et al., 2008), is dispensable for its association with ErbB4 (Figure 3A–3C). DOCK7 still interacted with a kinase-dead ErbB4 mutant (ErbB4-K751M; KD), but not a C-terminally truncated ErbB4 mutant (ErbB4ΔC) lacking most of the intracellular domain of ErbB4 (Figure 3B), indicating that DOCK7 binding requires the C-terminal cytoplasmic domain of ErbB4, but not its kinase activity. In accordance, DOCK7 associated with a fragment encoding just the cytoplasmic (C) domain of ErbB4 (Figure 3B).

While initially we envisioned DOCK7 to be primarily involved in mediating ErbB4 signaling, we surprisingly found that DOCK7 plays a prominent role in the activation of ErbB4. The first hint for this came from our observation that when DOCK7 or DOCK7ΔDHR2 was coexpressed with ErbB4 in Neuro 2A cells, tyrosine phosphorylation of immunoprecipitated ErbB4 was consistently increased compared to the empty control vector condition (Figure 3D). Notably, ErbB4, like all ErbB family members is subject to ligand-independent tyrosine phosphorylation when ectopically expressed (Nagy et al., 2010). To extend the above finding, we examined the effect of ectopic DOCK7 expression on ErbB4 autophosphorylation in Neuro 2A cells transiently expressing ErbB4 using a phospho-specific antibody that recognizes ErbB4 autophosphorylation at Tyr-1284. DOCK7 overexpression significantly increased the phosphorylation of wild-type, but not kinase-dead, ErbB4 (Figure 3E). We observed a similar increase in ErbB4 phosphorylation when DOCK7ΔDHR2 was ectopically expressed, indicating that DOCK7-induced ErbB4 activation does not require its GEF activity (Figure 3E, right panel).

We then examined whether conversely knockdown of DOCK7 diminishes ErbB4 activation by coexpressing the above-described Dock7 shRNAs with ErbB4 into Neuro 2A cells. Both Dock7#1 and Dock7#2 shRNA, but not scr#1 shRNA, significantly reduced ErbB4 autophosphorylation (Figure 3F). We further investigated the impact of DOCK7 knockdown on the activation of endogenously expressed ErbB4. Since we were unable to detect expression of endogenous ErbB4 in Neuro 2A cells, we resorted to a culture of primary subcortical neurons, in which ErbB4 expression was readily detected. These neurons were infected with a lentivirus expressing scr#1 or Dock7#2 shRNA, and the infected neurons as well as uninfected neurons (no) were either left unstimulated or stimulated with the ErbB4 ligand neuregulin-1 (NRG1) and analyzed for ErbB4 autophosphorylation. As expected, NRG1 treatment elicited a significant increase in ErbB4 phosphorylation in uninfected cells and in cells expressing scr#1 shRNA (Figure 3G). This increase was significantly reduced in cells expressing Dock7#2 shRNA (Figure 3G). Thus, these data corroborate the involvement of DOCK7 in the activation of ErbB4.

Finally, we determined whether DOCK7 could directly activate ErbB4. To this end, we performed an in vitro phosphorylation assay using commercially available purified ErbB4 protein and recombinant full-length DOCK7 protein produced in Sf9 insect cells or obtained from transiently transfected HEK293T cells. When DOCK7 was added at increasing amounts to the reaction buffer containing ErbB4, a dose-dependent increase in ErbB4 tyrosine phosphorylation was observed (Figures 3H and S4A), demonstrating that DOCK7 can indeed directly activate ErbB4. Together, these data indicate that DOCK7 acts as a cytoplasmic activator of ErbB4.

DOCK7 Modulates ErbB4 Activity to Regulate ChC Cartridge/Bouton Development

Next, we investigated the role and importance of DOCK7-mediated ErbB4 activation in ChC cartridge/bouton development. To approach this, we first examined the consequences of enhanced and reduced ErbB4 activity/expression on ChC cartridge/bouton development in our experimental system. For the former, we used a previously described ErbB4 mutant, ErbB4-E836K, which has been shown to display enhanced kinase activity (Prickett et al., 2009). For the latter, we used a previously described ErbB4 shRNA (ErbB4#2) (Li et al., 2007), which we confirmed to be effective in reducing ErbB4 protein levels (Figure S4C).

E12.5 embryos were coelectroporated with vectors expressing EGFP and ErbB4-E836K, ErbB4#2 shRNA, or corresponding control vectors, and brain slices were prepared and analyzed at P28 as described above. We observed that in ErbB4-E836K expressing cells the cartridges formed a well-organized network, while in ErbB4#2 shRNA-expressing cells they appeared less organized (Figures 4A, 4B, 4G, and 4H). Moreover, the density and size of ChC boutons were increased and decreased, respectively, in ErbB4-E836K and ErbB4#2 shRNA-transfected ChCs compared to those in the control groups (Figures 4E, 4F, 4K, and 4L). Thus, the phenotypes produced by ErbB4 gain- and loss-of-function variants in ChCs largely resemble those of DOCK7 gain- and loss-of-function, consistent with the idea that DOCK7 could control ChC cartridge/bouton development via ErbB4-mediated signaling.

To further establish this, we examined whether coexpression of ErbB4-E836K with Dock7#2 shRNA could overcome the ChC cartridge/bouton phenotypes evoked by DOCK7 RNAi and, conversely, whether coexpression of ErbB4#2 shRNA with Flag-DOCK7 could counteract the phenotypes elicited by ectopic DOCK7 expression. We found that ErbB4-E836K was

(G) Knockdown of DOCK7 decreases autophosphorylation of endogenously expressed ErbB4 in cultured subcortical neurons. Cultured subcortical neurons were left uninfected (no) or were infected with lentivirus expressing scr#1 or Dock7#2 shRNA and left unstimulated (−) or stimulated (+) with neuregulin-1 (NRG1) for 5 min. Cell extracts were prepared and subjected to western blot analysis with indicated Abs.

(H) DOCK7 enhances ErbB4 phosphorylation in a cell-free system. Recombinant ErbB4-Myc protein (20 ng) was incubated with increasing amounts of recombinant Flag/His6-DOCK7 protein (generated in insect cells) in the absence (−) or presence (+) of ATP for 30 min at 30°C. The reaction was terminated by addition of Laemmli buffer, and proteins were subjected to western blot analysis with the indicated Abs.

The numbers below (E)–(H) represent changes (n-fold) in signal intensities of PY20 or pErbB4 normalized to those of total ErbB4 and then to the value of 1.0 for the control condition. Numbers are the average of three to four independent experiments.

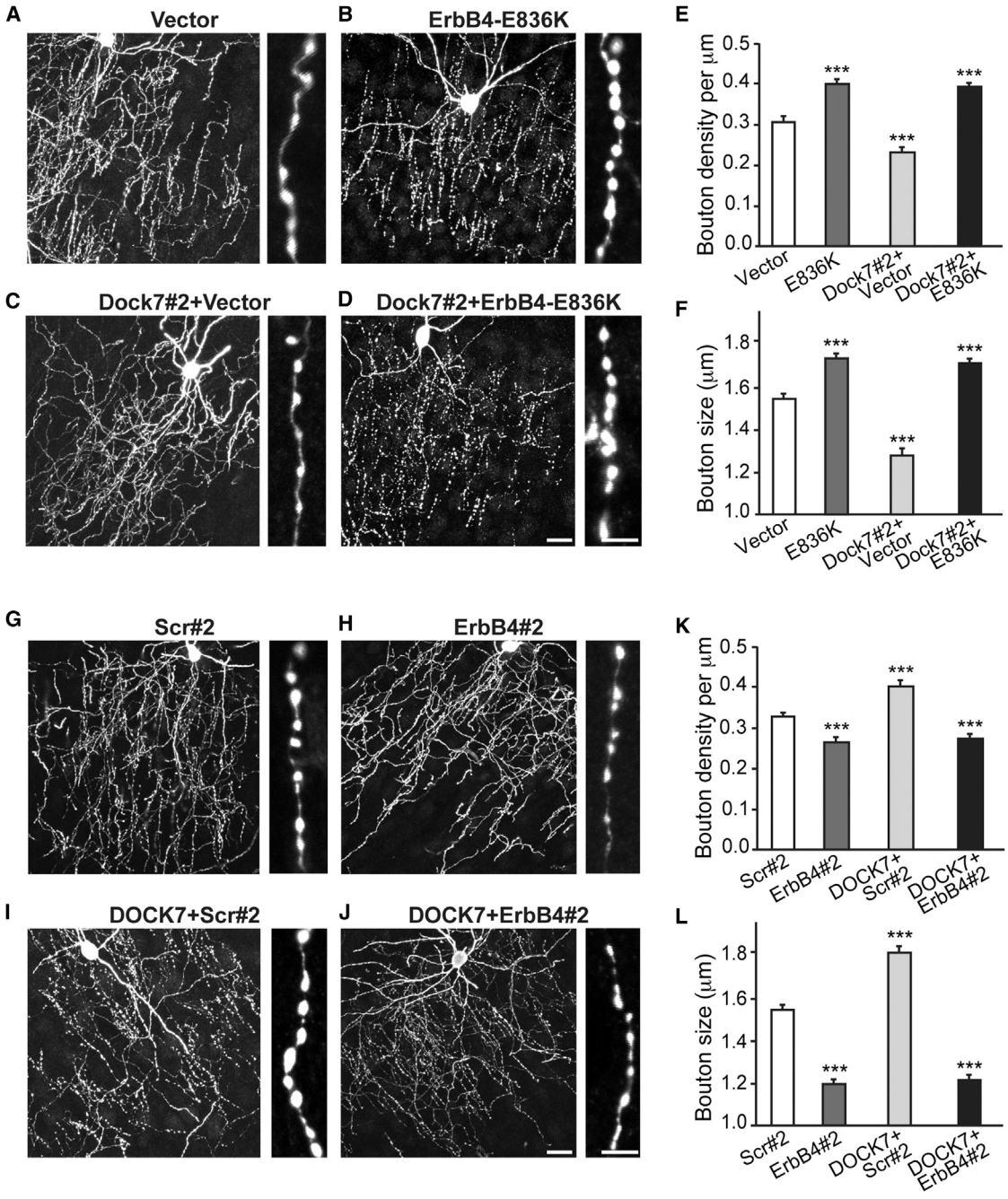

Figure 4. DOCK7 Regulates ChC Cartridge/Bouton Development by Modulating ErbB4 Activity

(A–D) Representative images of ChCs in layer II/III of somatosensory cortex from mice coelectroporated at E12.5 with plasmids expressing EGFP and empty control vector, ErbB4-E836K, Dock7#2 shRNA + vector, or Dock7#2 shRNA + ErbB4-E836K and sacrificed at P28. Enlarged view of ChC cartridges with boutons is depicted on the right. Scale bars, 20 μm (left) and 5 μm (right).

(E and F) Quantification of bouton density (E) and size (F). Data are mean ± SEM; 10–11 ChCs from three animals were analyzed for each condition, and for each cell 7–20 cartridges (E) and 90–162 boutons (F) were analyzed. ***$p < 0.001$, in comparison to vector; one-way ANOVA, post hoc Tukey-Kramer test.

(G–J) Representative images of ChCs in layer II/III of somatosensory cortex from mice coelectroporated at E12.5 with plasmids expressing EGFP and scr#2 shRNA, ErbB4#2 shRNA, Flag-DOCK7 + scr#2 shRNA, or Flag-DOCK7 + ErbB4#2 shRNA and sacrificed at P28. Enlarged view of ChC cartridges with boutons is depicted on the right. Scale bars, 20 μm (left) and 5 μm (right).

(K and L) Quantification of bouton density (K) and size (L). Data are mean ± SEM; 9–17 ChCs from three animals were analyzed for each condition, and for each cell 7–17 cartridges (K) and 91–158 boutons (L) were analyzed. ***$p < 0.001$, in comparison to scr#2; one-way ANOVA, post hoc Tukey-Kramer test.

able to overcome the decrease in bouton size and density, as well as cartridge disorganization, produced by DOCK7 RNAi (Figures 4C–4F), while ErbB4#2 shRNA prevented the increase in bouton size and density triggered by ectopic DOCK7 expression (Figures 4I–4L). Together with our biochemical data, these findings support a model in which DOCK7 modulates ErbB4 activity to regulate ChC cartridge/bouton development.

DISCUSSION

In this study, we describe an in utero electroporation-based method to fluorescently label single ChCs and manipulate gene expression in these cells. This approach enabled us to monitor ChCs at high cellular resolution, providing insights into ChC cartridge innervation of the AIS, and, significantly, leading to the identification of DOCK7 as a key regulator of ChC cartridge/bouton development. We further found that DOCK7, independent of its GEF activity, acts as a cytoplasmic activator of the RTK ErbB4, and importantly that DOCK7 promotes ChC cartridge/bouton development by enhancing ErbB4 activation.

ChCs so far have been identified only in mammals and found to be located in the neocortex, archicortex (i.e., hippocampus, piriform cortex), and amygdala (DeFelipe et al., 1985; Inda et al., 2009; McDonald, 1982; Sik et al., 1993; Somogyi et al., 1982). The developmental origin of ChCs in these three brain regions has been long sought after. Recent studies unveiled the vMGE and the ventral germinal zone (VGZ), likely a remnant or extension of the medial ganglionic eminence (MGE), as a source of neocortical ChCs, with the production of ChCs being noted as early as E13.5, increasing at E15, and reaching a peak at about E16 when the MGE has disappeared morphologically and the VGZ has emerged (Inan et al., 2012; Taniguchi et al., 2013). As to the origin of ChCs in the hippocampus and amygdala, this remains largely elusive. Intriguingly, by applying vMGE-directed in utero electroporation to developing mouse embryos (stages E12.5–E13.5), we were able to sparsely, but reproducibly, target gene expression in ChCs in all of the above three brain areas. Notably, we chose E12.5–E13.5, because at this stage the proliferative zone of the vMGE is directly adjacent to the lateral ventricle and hence readily accessible for gene transfer from that site. We infer from these data that a common pool or potentially distinct pools of ChC progenitors for the hippocampus, amygdala, and neocortex exist(s) from midgestation in the vMGE and that these progenitors then likely become competent in a temporally regulated manner to give rise to ChCs in the different brain regions. Future studies will, however, be required to further determine that this is the case.

Taking advantage of the versatility of electroporation to alter gene expression and the fact that ChCs are sparsely labeled by vMGE-directed in utero electroporation, we were able to demonstrate that normal DOCK7 expression within individual ChCs is essential for the proper development of ChC cartridges and boutons. Indeed, knockdown of DOCK7 in ChCs in cortical regions resulted in a disorganized network of ChC cartridges and a reduction in the number and size of boutons, while ectopic expression of DOCK7 brought about the opposite phenotypes. Our findings further indicate that other DOCK180 family members do not compensate for this function of DOCK7, as knockdown of DOCK7 alone is sufficient to cause defects in ChC cartridge/bouton development. It is noteworthy that previous studies had implicated DOCK7 function in Schwann cell myelination (Yamauchi et al., 2008) and the polarization (Watabe-Uchida et al., 2006) and genesis of newborn pyramidal neurons (Yang et al., 2012). While DOCK7 was shown to regulate these processes via its interaction with Rac1/Cdc42 GTPases (Watabe-Uchida et al., 2006; Yamauchi et al., 2008) or the centrosome- and microtubule-associated protein TACC3 (Yang et al., 2012), we found here that DOCK7 controls ChC cartridge/bouton development via its interaction with ErbB4 (see further below). Combined, these findings imply that DOCK7 exerts specific yet distinct roles in different cell types and does so by engaging in different protein-protein interactions. In this regard, multiple and nonredundant functions, often cell-type specific, have previously been demonstrated for several DOCK180 family members (Chen et al., 2009; Fukui et al., 2001; Laurin et al., 2008; Miyamoto and Yamauchi, 2010; Randall et al., 2011; Vives et al., 2011).

The first clue toward the mechanism by which DOCK7 controls ChC cartridge/bouton development came from our findings that DOCK7 interacts with the cytoplasmic domain of ErbB4 and, importantly, that it functions as a cytoplasmic activator of ErbB4. Indeed, we found that DOCK7 knockdown decreases and ectopic DOCK7 expression enhances ErbB4 activation. This function of DOCK7 does not require its catalytic DHR2 domain, indicating that DOCK7 enhances ErbB4 activation independently of its GEF activity. Noteworthy, so far only two other cytoplasmic activators of RTKs have been described. One is the adaptor protein Dok7, which activates the muscle-specific RTK MuSK and controls neuromuscular junction formation (Bergamin et al., 2010; Yamanashi et al., 2012). The other is the ARF-GEF ARNO, which enhances the activation of the EGFR and promotes the proliferation of EGFR-dependent tumor cells (Bill et al., 2010).

The importance of ErbB4 activation for DOCK7 function in ChC differentiation is supported by several of our findings. For starters, the phenotypes elicited by ErbB4 gain- and loss-of-function variants in ChCs largely resemble those of DOCK7 gain and loss of function. More importantly, we found that an ErbB4 mutant with enhanced kinase activity was able to overcome the phenotypes associated with DOCK7 knockdown. Conversely, silencing of ErbB4 prevented the phenotypes elicited by DOCK7 overexpression. Together with our biochemical data, these findings support a model in which DOCK7 controls ChC cartridge/bouton development by modulating ErbB4 activity and thereby its downstream signaling. What signaling pathway(s) mediate the effects of DOCK7/ErbB4 on ChC cartridge/bouton development remains an open question to be addressed in the future. Of interest is our finding that DOCK7 itself becomes tyrosine phosphorylated by ErbB4 (see Figure S4B), raising the possibility that a positive feedback loop exists, with DOCK7 enhancing ErbB4 activation and the latter in turn priming DOCK7 function; e.g., by facilitating DOCK7 recruitment to the membrane and/or eliciting a conformational change in DOCK7.

In summary, this study demonstrates the successful use of an in utero electroporation-based method to identify the

molecular mechanisms that govern the morphological differentiation of ChCs. We uncovered a critical role for DOCK7 as a cytoplasmic activator of ErbB4 in the regulation of ChC cartridge/bouton development. A key feature of defective DOCK7/ErbB4 signaling is a decrease in the number and size of ChC boutons, which interestingly is one of the most salient features of individuals with schizophrenia (Pierri et al., 1999; Woo et al., 1998). We envisage that such morphological changes are likely to impact the physiological properties of ChCs and, consequently, alter cortical network activity (Szabadics et al., 2006; Woodruff et al., 2011), which is thought to contribute to the cognitive abnormalities characteristic of schizophrenia (Lewis, 2012).

EXPERIMENTAL PROCEDURES

DNA and RNAi constructs, cell culture, and methods for transfection and viral infection are included in the Supplemental Experimental Procedures.

In Utero Electroporation

Timed-pregnant CD1 mice (Charles River) at 12.5 or 13.5 days of gestation were anesthetized, the uterine horns were exposed, and 1 to 2 μl of DNA solution (final concentration 1 μg/μl) was injected manually into the lateral ventricle of the embryos using a beveled glass micropipette. Custom-made tweezer electrodes were placed at about 60° from the brain's horizontal plane so as to direct the current toward the vMGE. Electric pulses (35 V; 50 ms) were passed five times at 1 s intervals using an electroporator (BTX, ECM830). After electroporation, the uterus was placed back in the abdominal cavity and the wound surgically sutured. Embryos were allowed to develop normally, and animals were sacrificed at P28, when ChCs are fully differentiated. ChCs were sparsely labeled using this method (approximately three to six cells in somatosensory cortex). Of note, the number of other interneurons targeted in the somatosensory cortex was more variable, ranging from 20 to 80. All animal care protocols were approved by CSHL.

Confocal Image Acquisition and Analysis

Images were acquired using a confocal microscope (Zeiss) with a 63× oil-immersion objective. Sequential acquisition settings were applied at the resolution of 2,048 × 2,048. Each image was a z series of 30–40 images at 1 μm depth interval. The resultant z stack was "flattened" into a single image using maximal projection. ChC cartridges were randomly chosen within a 150-μm-diameter circle centered on the cell body, and varicosities (boutons) were labeled with NeuroLucida software. Bouton density was determined by measuring cartridge length and counting the number of varicosities on each cartridge and represented as the number of varicosities divided by cartridge length. Bouton size was determined by measuring the diameter of a bouton parallel to the ChC axon using Zeiss LSM software. Preparation of brain slices and immunohistochemistry staining methods are described in the Supplemental Experimental Procedures.

Biochemical Analysis

Western blotting, coimmunoprecipitations, protein purification, and in vitro ErbB4 phosphorylation assay were performed largely as described elsewhere (Bill et al., 2010; Yamauchi et al., 2008; Yang et al., 2012). See the Supplemental Experimental Procedures for details.

Statistical Analysis

Data are presented as mean ± SEM from at least three independent experiments. Direct comparisons were made using Student's t test and multiple group comparisons using one-way analysis of variance (ANOVA) with a post hoc Tukey-Kramer multiple comparison test. Statistical significance was defined as $p < 0.01$ or 0.001 (indicated as ** or ***, respectively). p values $\geq$ 0.05 were considered not significant.

SUPPLEMENTAL INFORMATION

Supplemental information includes Supplemental Experimental Procedures and four figures and can be found with this article online at http://dx.doi.org/10.1016/j.celrep.2013.12.034.

ACKNOWLEDGMENTS

We thank Z.J. Huang, members of the L.V.A. lab, J. Skowronski, and E-.E. Govek for discussions and/or critical reading of the manuscript. We also thank Y-.T. Yang and S. Mitra Uyaniker for technical assistance. This work was supported by National Institutes of Health (NIH) grants R01 MH082808 and R01 NS082266 to L.V.A. C.-L.W. is supported by NIH grant T32 CA148056-1.

Received: August 15, 2013
Revised: November 1, 2013
Accepted: December 20, 2013
Published: January 16, 2014

REFERENCES

Batista-Brito, R., and Fishell, G. (2009). The developmental integration of cortical interneurons into a functional network. Curr. Top. Dev. Biol. *87*, 81–118.

Bergamin, E., Hallock, P.T., Burden, S.J., and Hubbard, S.R. (2010). The cytoplasmic adaptor protein Dok7 activates the receptor tyrosine kinase MuSK via dimerization. Mol. Cell *39*, 100–109.

Bill, A., Schmitz, A., Albertoni, B., Song, J.N., Heukamp, L.C., Walrafen, D., Thorwirth, F., Verveer, P.J., Zimmer, S., Meffert, L., et al. (2010). Cytohesins are cytoplasmic ErbB receptor activators. Cell *143*, 201–211.

Birchmeier, C. (2009). ErbB receptors and the development of the nervous system. Exp. Cell Res. *315*, 611–618.

Chen, Q., Peto, C.A., Shelton, G.D., Mizisin, A., Sawchenko, P.E., and Schubert, D. (2009). Loss of modifier of cell adhesion reveals a pathway leading to axonal degeneration. J. Neurosci. *29*, 118–130.

Côté, J.F., and Vuori, K. (2002). Identification of an evolutionarily conserved superfamily of DOCK180-related proteins with guanine nucleotide exchange activity. J. Cell Sci. *115*, 4901–4913.

DeFelipe, J. (1999). Chandelier cells and epilepsy. Brain *122*, 1807–1822.

DeFelipe, J., Hendry, S.H., Jones, E.G., and Schmechel, D. (1985). Variability in the terminations of GABAergic chandelier cell axons on initial segments of pyramidal cell axons in the monkey sensory-motor cortex. J. Comp. Neurol. *231*, 364–384.

Del Pino, I., García-Frigola, C., Dehorter, N., Brotons-Mas, J.R., Alvarez-Salvado, E., Martínez de Lagrán, M., Ciceri, G., Gabaldón, M.V., Moratal, D., Dierssen, M., et al. (2013). Erbb4 deletion from fast-spiking interneurons causes schizophrenia-like phenotypes. Neuron *79*, 1152–1168.

Fazzari, P., Paternain, A.V., Valiente, M., Pla, R., Luján, R., Lloyd, K., Lerma, J., Marín, O., and Rico, B. (2010). Control of cortical GABA circuitry development by Nrg1 and ErbB4 signalling. Nature *464*, 1376–1380.

Fish, K.N., Hoftman, G.D., Sheikh, W., Kitchens, M., and Lewis, D.A. (2013). Parvalbumin-containing chandelier and basket cell boutons have distinctive modes of maturation in monkey prefrontal cortex. J. Neurosci. *33*, 8352–8358.

Fukui, Y., Hashimoto, O., Sanui, T., Oono, T., Koga, H., Abe, M., Inayoshi, A., Noda, M., Oike, M., Shirai, T., and Sasazuki, T. (2001). Haematopoietic cell-specific CDM family protein DOCK2 is essential for lymphocyte migration. Nature *412*, 826–831.

Howard, A., Tamas, G., and Soltesz, I. (2005). Lighting the chandelier: new vistas for axo-axonic cells. Trends Neurosci. *28*, 310–316.

Huang, Z.J., Di Cristo, G., and Ango, F. (2007). Development of GABA innervation in the cerebral and cerebellar cortices. Nat. Rev. Neurosci. *8*, 673–686.

Inan, M., Welagen, J., and Anderson, S.A. (2012). Spatial and temporal bias in the mitotic origins of somatostatin- and parvalbumin-expressing interneuron

subgroups and the chandelier subtype in the medial ganglionic eminence. Cereb. Cortex *22*, 820–827.

Inan, M., Blázquez-Llorca, L., Merchán-Pérez, A., Anderson, S.A., DeFelipe, J., and Yuste, R. (2013). Dense and overlapping innervation of pyramidal neurons by chandelier cells. J. Neurosci. *33*, 1907–1914.

Inda, M.C., DeFelipe, J., and Muñoz, A. (2009). Morphology and distribution of chandelier cell axon terminals in the mouse cerebral cortex and claustroamygdaloid complex. Cereb. Cortex *19*, 41–54.

Laurin, M., Fradet, N., Blangy, A., Hall, A., Vuori, K., and Côté, J.F. (2008). The atypical Rac activator Dock180 (Dock1) regulates myoblast fusion in vivo. Proc. Natl. Acad. Sci. USA *105*, 15446–15451.

Lewis, D.A. (2012). Cortical circuit dysfunction and cognitive deficits in schizophrenia—implications for preemptive interventions. Eur. J. Neurosci. *35*, 1871–1878.

Li, B., Woo, R.S., Mei, L., and Malinow, R. (2007). The neuregulin-1 receptor erbB4 controls glutamatergic synapse maturation and plasticity. Neuron *54*, 583–597.

Marín, O. (2012). Interneuron dysfunction in psychiatric disorders. Nat. Rev. Neurosci. *13*, 107–120.

McDonald, A.J. (1982). Neurons of the lateral and basolateral amygdaloid nuclei: a Golgi study in the rat. J. Comp. Neurol. *212*, 293–312.

Meller, N., Merlot, S., and Guda, C. (2005). CZH proteins: a new family of Rho-GEFs. J. Cell Sci. *118*, 4937–4946.

Miyamoto, Y., and Yamauchi, J. (2010). Cellular signaling of Dock family proteins in neural function. Cell. Signal. *22*, 175–182.

Nagy, P., Claus, J., Jovin, T.M., and Arndt-Jovin, D.J. (2010). Distribution of resting and ligand-bound ErbB1 and ErbB2 receptor tyrosine kinases in living cells using number and brightness analysis. Proc. Natl. Acad. Sci. USA *107*, 16524–16529.

Ogawa, Y., and Rasband, M.N. (2008). The functional organization and assembly of the axon initial segment. Curr. Opin. Neurobiol. *18*, 307–313.

Pierri, J.N., Chaudry, A.S., Woo, T.U., and Lewis, D.A. (1999). Alterations in chandelier neuron axon terminals in the prefrontal cortex of schizophrenic subjects. Am. J. Psychiatry *156*, 1709–1719.

Prickett, T.D., Agrawal, N.S., Wei, X., Yates, K.E., Lin, J.C., Wunderlich, J.R., Cronin, J.C., Cruz, P., Rosenberg, S.A., and Samuels, Y. (2009). Analysis of the tyrosine kinome in melanoma reveals recurrent mutations in ERBB4. Nat. Genet. *41*, 1127–1132.

Randall, K.L., Chan, S.S., Ma, C.S., Fung, I., Mei, Y., Yabas, M., Tan, A., Arkwright, P.D., Al Suwairi, W., Lugo Reyes, S.O., et al. (2011). DOCK8 deficiency impairs CD8 T cell survival and function in humans and mice. J. Exp. Med. *208*, 2305–2320.

Sik, A., Tamamaki, N., and Freund, T.F. (1993). Complete axon arborization of a single CA3 pyramidal cell in the rat hippocampus, and its relationship with postsynaptic parvalbumin-containing interneurons. Eur. J. Neurosci. *5*, 1719–1728.

Somogyi, P. (1977). A specific 'axo-axonal' interneuron in the visual cortex of the rat. Brain Res. *136*, 345–350.

Somogyi, P., Freund, T.F., and Cowey, A. (1982). The axo-axonic interneuron in the cerebral cortex of the rat, cat and monkey. Neuroscience *7*, 2577–2607.

Szabadics, J., Varga, C., Molnár, G., Oláh, S., Barzó, P., and Tamás, G. (2006). Excitatory effect of GABAergic axo-axonic cells in cortical microcircuits. Science *311*, 233–235.

Taniguchi, H., Lu, J., and Huang, Z.J. (2013). The spatial and temporal origin of chandelier cells in mouse neocortex. Science *339*, 70–74.

Vives, V., Laurin, M., Cres, G., Larrousse, P., Morichaud, Z., Noel, D., Côté, J.F., and Blangy, A. (2011). The Rac1 exchange factor Dock5 is essential for bone resorption by osteoclasts. J. Bone Miner. Res. *26*, 1099–1110.

Watabe-Uchida, M., John, K.A., Janas, J.A., Newey, S.E., and Van Aelst, L. (2006). The Rac activator DOCK7 regulates neuronal polarity through local phosphorylation of stathmin/Op18. Neuron *51*, 727–739.

Woo, T.U., Whitehead, R.E., Melchitzky, D.S., and Lewis, D.A. (1998). A subclass of prefrontal gamma-aminobutyric acid axon terminals are selectively altered in schizophrenia. Proc. Natl. Acad. Sci. USA *95*, 5341–5346.

Woodruff, A.R., Anderson, S.A., and Yuste, R. (2010). The enigmatic function of chandelier cells. Front. Neurosci. *4*, 201.

Woodruff, A.R., McGarry, L.M., Vogels, T.P., Inan, M., Anderson, S.A., and Yuste, R. (2011). State-dependent function of neocortical chandelier cells. J. Neurosci. *31*, 17872–17886.

Yamanashi, Y., Tezuka, T., and Yokoyama, K. (2012). Activation of receptor protein-tyrosine kinases from the cytoplasmic compartment. J. Biochem. *151*, 353–359.

Yamauchi, J., Miyamoto, Y., Chan, J.R., and Tanoue, A. (2008). ErbB2 directly activates the exchange factor Dock7 to promote Schwann cell migration. J. Cell Biol. *181*, 351–365.

Yang, Y.T., Wang, C.L., and Van Aelst, L. (2012). DOCK7 interacts with TACC3 to regulate interkinetic nuclear migration and cortical neurogenesis. Nat. Neurosci. *15*, 1201–1210.